Nonlinear Responses of Sloshing Based on the Shallow Water Wave Theory*

Takashi SHIMIZU** and Shinji HAYAMA***

Based on the shallow water wave theory, the basic equations to describe the nonlinear responses of sloshing are derived, and a numerical method is presented to simulate sloshing phenomena in a rectangular tank which is oscillated horizontally. As the dispersion relation of the free surface wave plays an important role in the stable calculation of resonant responses, it should thus be taken into consideration. In this study, it is implicitly replaced by the dispersion relation produced by the discretization of the basic equations. Numerical results are in good agreement with those of experiments. In cases of shallow water depths, stable progressive waves are observed both in experiments and in numerical calculations, and the various nonlinear characteristics of sloshing, such as the hardening restoring forces and the jumping phenomena in resonant responses are well-simulated by the basic equations and the calculation method presented in this paper.

Key Words: Fluid Vibration, Sloshing, Nonlinear Response, Shallow Water Wave, Dispersion Relation, Numerical Simulation

1. Introduction

Sloshing phenomena or free surface oscillations of liquids in a tank caused by huge earthquakes are very important problems which require clarification in their connection with hazard prevention. Many studies have been done on the sloshing problems in liquid tanks. Natural frequencies of sloshing have been obtained for various types of tanks[1][2]. The nonlinear responses of the free surface elevation have also been studied for various cases[3]~[9].

The depth of the liquid in a large-sized tank is considered to be small compared with its horizontal representative length. So, sloshing phenomena in such a tank are often in the range of the shallow water wave theory, and show nonlinear characteristics beyond the linear wave theory with an infinitesimal amplitude. It is estimated that nonlinear waves, such as solitary or cnoidal waves[10][11], might have occurred in various oil-storage tanks which have experienced an overflow of oil during earthquakes. Few studies, however, have been done on these problems.

In this paper, the basic equations for describing the nonlinear responses of sloshing are first derived, and a numerical method is then presented to simulate the nonlinear sloshing phenomena in a rectangular tank which is forced to oscillate harmonically in the horizontal direction.

2. Nomenclature

a : nondimensional amplitude of tank oscillation
g : acceleration of gravity
H : depth of stationary liquid
k : wave number
k_1 : reference wave number
n : number of divisions in x-direction
$o-xyz$: coordination system fixed with tank
p : pressure
$q^2=u^2+v^2+w^2$
R : half of tank width in x-direction
t : time
u, v, w : flow velocities in x-, y-, and z-directions,

* Received 18th December, 1986. Paper No. 86-0385A
** Toyota Motor Co., Toyota-cho 1, Toyota, Aichi, 471, Japan
*** Department of Mechanical Engineering, University of Tokyo, 7-3-1 Hongo, Bunkyo, Tokyo, 113, Japan

respectively
u_s, v_s : flow velocities in x- and y-directions on free surface
X_G, Y_G : tank displacements in x- and y-directions
δ : ratio of liquid depth to half of tank width
Δx : width of control volume in x-direction
η : surface elevation
λ : damping coefficient
ρ : density of liquid
τ : number of harmonically forced tank displacements
Φ : velocity potential
ω : forcing angular frequency of tank displacement
ω_m : m-th order natural angular frequency

3. Basic Equations of Sloshing

3.1 Derivation of basic equations

The basic equations for describing the nonlinear responses of sloshing in a tank under horizontal oscillation are derived, referring to the shallow water wave theory[10]. The derivation in this chapter deals with three-dimensional flow in a tank, a special case of which represents two-dimensional flow in a rectangular tank.

As shown in Fig.1, a coordinate system fixed with the tank is set in such a way that the origin is located in the center of the stationary liquid surface, and that the x-and z-axes are chosen in the horizontal and vertical directions, respectively, and the y-axis perpendicular to the xz-plane.

Let H be the depth of a stationary liquid in a tank of width $2R$ in the x-direction. The tank is subjected to harmonic displacements X_G and Y_G in the x- and y- directions, respectively. For simplification of the analysis, the following are assumed. (1) The liquid in the tank is incompressible, inviscid and irrotational. (2) Pressure is constant on the free surface. (3) The tank wall is rigid and the stationary liquid depth H is constant. Then, the equations of continuity and motion are expressed, respectively, as,

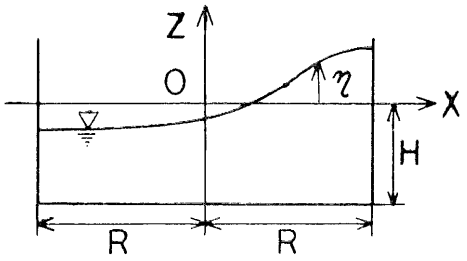

Fig. 1 A liquid tank and the coordinate system adopted.

$$\frac{\partial u}{\partial x}+\frac{\partial v}{\partial y}+\frac{\partial w}{\partial z}=0 \tag{1}$$

$$\left.\begin{aligned}
&\frac{\partial u}{\partial t}+u\frac{\partial u}{\partial x}+v\frac{\partial u}{\partial y}+w\frac{\partial u}{\partial z}=-\frac{1}{\rho}\frac{\partial p}{\partial x}-\ddot{X}_G\\
&\frac{\partial v}{\partial t}+u\frac{\partial v}{\partial x}+v\frac{\partial v}{\partial y}+w\frac{\partial v}{\partial z}=-\frac{1}{\rho}\frac{\partial p}{\partial y}-\ddot{Y}_G\\
&\frac{\partial w}{\partial t}+u\frac{\partial w}{\partial x}+v\frac{\partial w}{\partial y}+w\frac{\partial w}{\partial z}=-\frac{1}{\rho}\frac{\partial p}{\partial z}-g
\end{aligned}\right\} \tag{2}$$

where a dot denotes the derivative with respect to time.

Assumption (1) suggests the existence of a velocity potential Φ which satisfies the following Laplace's equation,

$$\Delta\Phi=0 \tag{3}$$

Assuming that the velocity potential Φ is expressed in the form of $\Phi=F(x, y, t)\,G(z)$, where F and G are arbitrary functions, and applying the boundary condition on the bottom wall of the tank, that is, $w=0$ at $z=-H$, Φ can be expressed as

$$\Phi=F(x, y, t)\cosh k(H+z) \tag{4}$$

From this, the velocity components u, v, w are obtained, as follows:

$$\left.\begin{aligned}
&u=\partial F/\partial x\cosh k(H+z)\\
&v=\partial F/\partial y\cosh k(H+z)\\
&w=kF\sinh k(H+z)\\
&u_s=\partial F/\partial x\cosh k(H+\eta)\\
&v_s=\partial F/\partial y\cosh k(H+\eta)
\end{aligned}\right\} \tag{5}$$

where k is a constant arising from the separation of variables and is called the wave number, and u_s and v_s are flow velocities in the x- and y-directions on the free surface, respectively. When k is given, the distributions of the flow velocity in the z- direction are known.

The following approximation will be employed in the analysis to be described, for the sake of simplicity,

$$\frac{\partial U_s}{\partial X}=\left(\frac{\partial U}{\partial X}\right)_{z=\eta}+\frac{\partial \eta}{\partial X}\left(\frac{\partial U}{\partial z}\right)_{z=\eta}\cong\left(\frac{\partial U}{\partial X}\right)_{z=\eta} \tag{6}$$

$(X=x,y,t,\ U=u,v,w,q)$

where the symbol $(\ )_{z=\eta}$ denotes that $z=\eta$ is substituted after the partial derivative of U with respect to X or z has been calculated.

Making use of Eqs.(5) and (6), the equations of continuity (1) and motion (2) are integrated with respect to z, from the bottom wall $z=-H$ to the free surface $z=\eta$, respectively. The integrations eliminate the independent variable z from the dependent variables, so we are left with a two-dimensional problem characterized by the dependent variables η, u_s and v_s.

Integration of Eq.(1) with respect to z yields

$$\frac{\partial \eta}{\partial t}+H\sigma\frac{\partial(\phi u_s)}{\partial x}+H\sigma\frac{\partial(\phi v_s)}{\partial y}=0 \tag{7}$$

where σ and ϕ are defined as follows.

$$\left.\begin{aligned}&\sigma=\tanh kH/(kH)\\&\phi(\eta/H)=T_H/\tanh kH\\&T_H(\eta/H)=\tanh kH(1+\eta/H)\end{aligned}\right\}\quad(8)$$

Next, integrating the third of Eqs.(2) with respect to z and choosing an integration constant so that $p=p_0$ at $z=\eta$, the following equation is obtained.

$$\frac{p-p_0}{\rho}=g(\eta-z)+\frac{q_s^2-q^2}{2}+\int_z^\eta\frac{\partial w}{\partial t}dz\quad(9)$$

Substituting Eq.(9) into the first and the second of Eqs.(2) in order to eliminate p, putting $z=\eta$, and rearranging them with the use of Eqs.(5) and (6), the following equations are obtained.

$$\left.\begin{aligned}&\frac{\partial u_s}{\partial t}+g\frac{\partial\eta}{\partial x}+\frac{1}{2}\frac{\partial q_s^2}{\partial x}+\frac{\partial\eta}{\partial x}\left(\frac{\partial w}{\partial t}\right)_{z=\eta}=-\ddot{X}_G\\&\frac{\partial v_s}{\partial t}+g\frac{\partial\eta}{\partial y}+\frac{1}{2}\frac{\partial q_s^2}{\partial y}+\frac{\partial\eta}{\partial y}\left(\frac{\partial w}{\partial t}\right)_{z=\eta}=-\ddot{Y}_G\end{aligned}\right\}\quad(10)$$

From Eqs.(1) and (5), the following is also obtained.

$$w=-\frac{1}{k}\left(\frac{\partial u}{\partial x}+\frac{\partial v}{\partial y}\right)\tanh k(H+z)\quad(11)$$

Elimination of w from Eqs.(10) by making use of Eq.(11) finally yields the following:

$$\begin{aligned}&\frac{\partial u_s}{\partial t}+g\frac{\partial\eta}{\partial x}+\frac{1-T_H^2}{2}\frac{\partial u_s^2}{\partial x}+\frac{1+T_H^2}{2}\frac{\partial v_s^2}{\partial x}\\&-T_H^2\frac{\partial(u_sv_s)}{\partial y}+gH\sigma\phi\left(\frac{\partial^2\eta}{\partial x^2}+\frac{\partial^2\eta}{\partial y^2}\right)\frac{\partial\eta}{\partial x}\\&=-\ddot{X}_G\end{aligned}\quad(12)$$

$$\begin{aligned}&\frac{\partial v_s}{\partial t}+g\frac{\partial\eta}{\partial y}+\frac{1+T_H^2}{2}\frac{\partial u_s^2}{\partial y}+\frac{1-T_H^2}{2}\frac{\partial v_s^2}{\partial y}\\&-T_H^2\frac{\partial(u_sv_s)}{\partial x}+gH\sigma\phi\left(\frac{\partial^2\eta}{\partial x^2}+\frac{\partial^2\eta}{\partial y^2}\right)\frac{\partial\eta}{\partial y}\\&=-\ddot{Y}_G\end{aligned}\quad(13)$$

Now, to rewrite Eqs.(7), (12), and (13) in nondimensional forms, the following nondimensional variables are introduced:

$$\left.\begin{aligned}&x^*=x/R,\ y^*=y/R,\ z^*=z/H,\ t^*=t/t_1\\&\eta^*=\eta/H,\ u^*=u/c,\ v^*=v/c,\ \Phi^*=\Phi/(cR)\\&X_G^*=X_G/R,\ Y_G^*=Y_G/R,\ k^*=kR\end{aligned}\right\}\quad(14)$$

Redefining σ_1 by a reference wave number k_1^*,

$$\delta=H/R,\ \sigma_1=\tanh k_1^*\delta/(k_1^*\delta)\quad(15)$$

then, t_1 and c in Eqs.(14) are given as,

$$t_1=R/\sqrt{gH\sigma_1},\ c=\sqrt{gH/\sigma_1}\quad(16)$$

Using these variables and parameters, Eqs.(7), (12), and (13) are expressed in nondimensional forms as

$$\begin{aligned}&\frac{\partial\eta^*}{\partial t^*}+\frac{\partial u_s^*}{\partial x^*}+\frac{\partial v_s^*}{\partial y^*}+\left(\frac{\sigma}{\sigma_1}-1\right)\left(\frac{\partial u_s^*}{\partial x^*}+\frac{\partial v_s^*}{\partial y^*}\right)\\&+\frac{\sigma}{\sigma_1}\left\{\frac{\partial(\phi-1)u_s^*}{\partial x^*}+\frac{\partial(\phi-1)v_s^*}{\partial y^*}\right\}=0\end{aligned}\quad(17)$$

$$\begin{aligned}&\frac{\partial u_s^*}{\partial t^*}+\frac{\partial\eta^*}{\partial x^*}+\frac{1-T_H^2}{2\sigma_1}\frac{\partial u_s^{*2}}{\partial x^*}+\frac{1+T_H^2}{2\sigma_1}\frac{\partial v_s^{*2}}{\partial x^*}\\&-\frac{T_H^2}{\sigma_1}\frac{\partial(u_s^*v_s^*)}{\partial y^*}+\sigma\phi\delta^2\left(\frac{\partial^2\eta^*}{\partial x^{*2}}+\frac{\partial^2\eta^*}{\partial y^{*2}}\right)\frac{\partial\eta^*}{\partial x^*}\\&=-\sigma_1\ddot{X}_G^*\end{aligned}\quad(18)$$

$$\begin{aligned}&\frac{\partial v_s^*}{\partial t^*}+\frac{\partial\eta^*}{\partial y^*}+\frac{1+T_H^2}{2\sigma_1}\frac{\partial u_s^{*2}}{\partial y^*}+\frac{1-T_H^2}{2\sigma_1}\frac{\partial v_s^{*2}}{\partial y^*}\\&-\frac{T_H^2}{\sigma_1}\frac{\partial(u_s^*v_s^*)}{\partial x^*}+\sigma\phi\delta^2\left(\frac{\partial^2\eta^*}{\partial x^{*2}}+\frac{\partial^2\eta^*}{\partial y^{*2}}\right)\frac{\partial\eta^*}{\partial y^*}\\&=-\sigma_1\ddot{Y}_G^*\end{aligned}\quad(19)$$

These three equations are the basic equations for describing the nonlinear sloshing phenomena in liquid tanks.From this point on, the superscripts * denoting nondimensional variables, and s identifying the values on the free surface are omitted for simplicity of description.

3.2 Dispersion relation

Elimination of the nonlinear terms and the forcing accelerations from Eqs.(17) through (19) yields

$$\left.\begin{aligned}&\frac{\partial\eta}{\partial t}+\frac{\partial u}{\partial x}+\frac{\partial v}{\partial y}+\left(\frac{\sigma}{\sigma_1}-1\right)\left(\frac{\partial u}{\partial x}+\frac{\partial v}{\partial y}\right)=0\\&\frac{\partial u}{\partial t}+\frac{\partial\eta}{\partial x}=0\quad\frac{\partial v}{\partial t}+\frac{\partial\eta}{\partial y}=0\end{aligned}\right\}\quad(20)$$

which represent the linear, free oscillations of the surface elevation. To obtain the dispersion relation or the relation between a wave number k and the corresponding circular frequency ω, the velocity potential is assumed to be expressed as

$$\Phi=f(x,y)e^{i\omega t}\cosh k\delta(1+z)\quad(21)$$

Assuming, again, that u and v in Eqs.(20) are the velocities at $z=0$, the following equation is obtained from Eqs.(20) and (21).

$$\frac{\partial^2 f}{\partial x^2}+\frac{\partial^2 f}{\partial y^2}+\omega^2\frac{\sigma_1}{\sigma}f=0\quad(22)$$

On the other hand, as Φ satisfies the Laplace's equation (3), the following is also obtained.

$$\frac{\partial^2 f}{\partial x^2}+\frac{\partial^2 f}{\partial y^2}+k^2f=0\quad(23)$$

Comparing Eqs.(22) and (23) with each other, the dispersion relation is obtained as

$$\omega=k\sqrt{\frac{\sigma}{\sigma_1}}\simeq k-\frac{\delta^2}{6}k^3\quad(24)$$

where the expanded approximation holds when $k\delta\ll1$. It is seen that the dispersion of free surface waves becomes weaker as δ becomes smaller.

3.3 Basic equations for a rectangular tank

In the following, only a rectangular tank is dealt with, and two-dimensional flow parallel to the xz-plane is assumed. Letting $v=0$ in Eqs.(17) through (19), the basic equations for a rectangular tank are expressed as follows.

$$\frac{\partial\eta}{\partial t}+\frac{\partial u}{\partial x}+\left(\frac{\sigma}{\sigma_1}-1\right)\frac{\partial u}{\partial x}+\frac{\sigma}{\sigma_1}\frac{\partial(\phi-1)u}{\partial x}=0\quad(25)$$

$$\begin{aligned}&\frac{\partial u}{\partial t}+\frac{\partial\eta}{\partial x}+\frac{1-T_H^2}{2\sigma_1}\frac{\partial u^2}{\partial x}+\sigma\phi\delta^2\frac{\partial^2\eta}{\partial x^2}\frac{\partial\eta}{\partial x}\\&=-\sigma_1\ddot{X}_G\end{aligned}\quad(26)$$

The boundary conditions on the side walls of the tank are given as $u=0$ on $x=1$ and $x=-1$. Solving Eq.(23) under these boundary conditions, wave numbers are determined as $k=m\pi/2$ (m is a positive integer). In this study, to calculate the responses of sloshing in the vicinity of the first order resonance, a reference wave

number k_1 is chosen as $k_1=\pi/2$.

4. Discretized Equations for a Rectangular Tank

In order to calculate the responses of sloshing in a rectangular tank, the basic equations are discretized into ordinary differential equations which will be solved numerically. Equations (25) and (26) are the equations for an arbitrary k. The free surface waves originally have a dispersion character which depends on k. If k_1 is substituted for k in Eq.(25), the so-called dispersion term, that is, the third one, disappears and the dispersion of free surface waves cannot then be taken into consideration. It is known[12], fortunately, that the discretization gives the dispersion character to the waves propagating through the discretized system. So, substituting k_1 for k in the basic equations (25) and (26), and eliminating the dispersion term, the original dispersion of free surface waves is replaced by that produced by the discretization. In this way, the dispersion character is implicitly taken into consideration.

4.1 Dispersion relation produced by discretization

Eliminating the nonlinear terms and the forcing acceleration from Eqs.(25) and (26) and setting $k=k_1$, the following equations are obtained.

$$\frac{\partial\eta}{\partial t}+\frac{\partial u}{\partial x}=0,\quad \frac{\partial u}{\partial t}+\frac{\partial\eta}{\partial x}=0 \tag{27}$$

The tank width of 2 is divided into n control volumes for u, and $n+1$ for η. In each control volume, the dependent variables $u_i(i=1\sim n)$ or $\eta_i(i=0\sim n)$ are arranged as shown in Fig.4. The width of a control volume is given as follows.

$$\Delta x=2/n \tag{28}$$

Integrating the first and the second of Eqs.(27) over the control volumes of η_i and u_i, respectively, the following equations are obtained.

$$\left.\begin{aligned}\frac{d\eta_i}{dt}&=\frac{1}{\Delta x}(u_i-u_{i+1})\\ \frac{du_i}{dt}&=\frac{1}{\Delta x}(\eta_{i-1}-\eta_i)\end{aligned}\right\} \tag{29}$$

Eliminating u_i from Eqs.(29) and substituting a general solution expressed in Eq.(30) into the resultant equation,

$$\eta_i=(\alpha\sin kx_i+\beta\cos kx_i)\sin(\omega t+\gamma)$$
(α, β, γ are constants.) (30)

the following is obtained:

$$\omega=\frac{2}{\Delta x}\sin\frac{k\Delta x}{2}=n\sin\frac{k}{n}\cong k-\frac{1}{6n^2}k^3 \tag{31}$$

where the expanded approximation holds when $k\ll n$. This is the dispersion relation produced by the discretization. It is seen that the dispersion becomes weaker as n becomes larger.

Now, it would be reasonable to determine the number of divisions, n, so that the dispersion relation of Eq.(31) can approximate that of Eq.(24). For this purpose, the following two methods are considered.

(1) In the case of $k\delta\ll 1$, the approximated expression of Eq.(31) is equated to that of Eq.(24). Then, the following relation is obtained.

$$n=1/\delta \tag{32}$$

(2) The ratio of the first order natural angular frequency $\omega_1(k_1=\pi/2)$ to the second order one $\omega_2(k_2=\pi)$, calculated from Eq.(31), is equated to that from Eq.(24). Then, the following relation is obtained.

$$n=\pi/\left\{2\ \text{are cos}\sqrt{\frac{\tanh\pi\delta}{2\tanh(\pi\delta/2)}}\right\} \tag{33}$$

In Fig.2 the relations between δ and n calculated from Eqs.(32) and (33) are plotted. It is seen that while Eq.(32) does not yield reasonable values of n for larger δ, Eq.(33) yields the limiting value of $n=2$.

In Fig. 3, the dispersion relations of Eq.(24) and

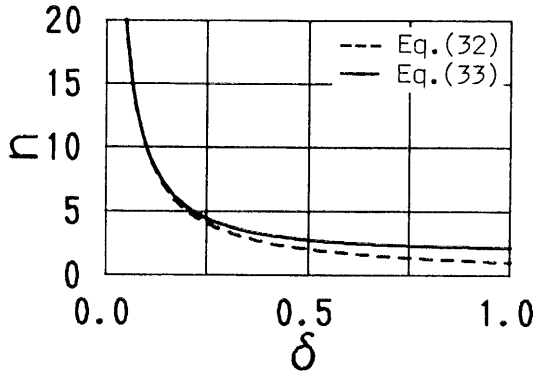

Fig. 2 The relations between δ and n.

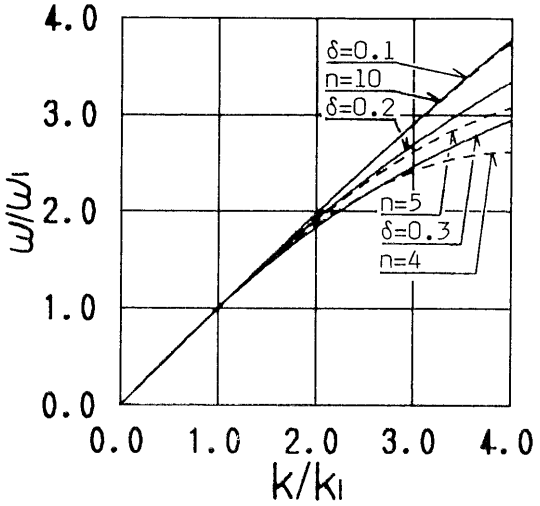

Fig. 3 The dispersion relations.

Eq.(31) are plotted, where, rounding off the values obtained by Eq.(33) to integers, the numbers of divisions are chosen as $n=10, 5$, and 4 for $\delta=0.1, 0.2$ and 0.3, respectively. It is seen that for larger values of k/k_1 or δ, the differences between Eqs.(24) and (31) become larger.

4.2 Discretization

Substituting k_1 for k in Eqs.(25) and (26), they can be rewritten as,

$$\frac{\partial\eta}{\partial t}+\frac{\partial(\phi u)}{\partial x}=0 \tag{34}$$

$$\frac{\partial u}{\partial t}+\frac{\partial\eta}{\partial x}+\frac{h}{2}\frac{\partial u^2}{\partial x}+C\frac{\partial^2\eta}{\partial x^2}\frac{\partial\eta}{\partial x}=-\sigma\ddot{X}_G \tag{35}$$

Now, omitting the subscript 1 to denote the values for $k=k_1$, the following constants and functions are redefined.

$$\left.\begin{aligned} &k_1=\pi/2,\quad \sigma=\tanh k_1\delta/(k_1\delta)\\ &\phi(\eta)=\tanh k_1\delta(1+\eta)/\tanh k_1\delta\\ &h(\eta)=\{1-(\phi\tanh k_1\delta)^2\}/\sigma\\ &C(\eta)=\sigma\phi\delta^2\\ &K(u)=u^2/2,\quad I(\eta)=(\partial\eta/\partial x)^2/2 \end{aligned}\right\} \tag{36}$$

Discretizing the tank width of 2, as shown in Fig.4, and integrating Eqs.(34) and (35) over the control volumes of η_i and u_i, respectively (in this case, the boundary conditions are applied for η_0 and η_n), the following equations are obtained.

$$\left.\begin{aligned} &\frac{d\eta_i}{dt}=\frac{1}{\Delta x}(\phi_i u_i-\phi_{i+1}u_{i+1})\\ &\quad(i=1\sim n-1)\\ &\frac{d\eta_0}{dt}=-\frac{2}{\Delta x}\phi_1 u_1\qquad \frac{d\eta_n}{dt}=\frac{2}{\Delta x}\phi_n u_n\\ &\frac{du_i}{dt}=\frac{1}{\Delta x}\{\eta_{i-1}-\eta_i+h_i(K_{i-1}-K_i)\\ &\qquad+C_i(I_{i-1}-I_i)\}-\sigma\ddot{X}_G\\ &\quad(i=1\sim n) \end{aligned}\right\} \tag{37}$$

where ϕ_i, h_i, C_i, K_i, and I_i are determined, assuming linear distributions of η_i and u_i over each control volume, as

$$\left.\begin{aligned} &\phi_i=\tanh k_1\delta\{1+(\eta_{i-1}+\eta_i)/2\}/\tanh k_1\delta\\ &h_i=\{1-(\phi_i\tanh k_1\delta)^2\}/\sigma\\ &C_i=\sigma\phi_i\delta^2\\ &\quad(i=1\sim n)\\ &K_i=\{(u_i+u_{i+1})/2\}^2/2\\ &I_i=\{(\eta_{i+1}-\eta_{i-1})/(2\Delta x)\}^2/2\\ &\quad(i=1\sim n-1)\\ &K_0=K_n=0\\ &I_0=\{(-3\eta_0+4\eta_1-\eta_2)/(2\Delta x)\}^2/2\\ &I_n=\{(\eta_{n-2}-4\eta_{n-1}+3\eta_n)/(2\Delta x)\}^2/2 \end{aligned}\right\} \tag{38}$$

For given initial conditions of η_i and u_i and a forcing tank displacement X_G, the simultaneous ordinary differential equations (37) are solved numerically, and the transient and steady responses of sloshing in a rectangular tank are obtained.

5. Experiments and Numerical Simulations

5.1 Experiments

The tank used in experiments was a rectangular open tank made of 1 cm-thick acrylic plate. Based on inside measurements, the tank was 100 cm wide, 35 cm high and 10 cm in the direction perpendicular to the xz-plane in Fig.1. It was placed on a vibrator-base for horizontal movement in the longitudinal direction. The liquid used was water, and the experiments were carried out at relatively shallow water depths. The tank was set in harmonic movement from a stationary liquid state, and the surface elevation was measured on a side wall. Transient responses of the surface elevation were measured with an electrostatic-capacity-type level gauge and recorded by a linear recorder. After the oscillations of the surface elevation had reached the steady state, their maximum and minimum values were measured by a scale attached on the side wall. The measurements were made in the vicinity of the first order resonance point with a constant amplitude of tank displacement, and the resonant responses of the surface elevation were thus obtained.

5.2 Numerical simulations

Numerical simulations were then carried out to predict the results obtained in the experiment. Adding the damping term $-\lambda u_i$ to the equation of u_i, Eqs.(37) are integrated by the Runge-Kutta-Gill Method. The values of the damping coefficient λ were chosen as $\lambda=0.06, 0.02$ and 0.01 for $\delta=0.1, 0.2$ and 0.3, respectively. The number of divisions, n, was determined for each δ by rounding off the value calculated from Eq.(33) to an integer. The time step used was 1/60 of one period of tank oscillation. The nondimensional tank displacement is expressed as

$$X_G=a\sin\omega t \tag{39}$$

where ω is a nondimensional forcing angular frequency. A non-dimensional forcing amplitude, a, was chosen as $a=0.005$ for all cases. Finally, the number of

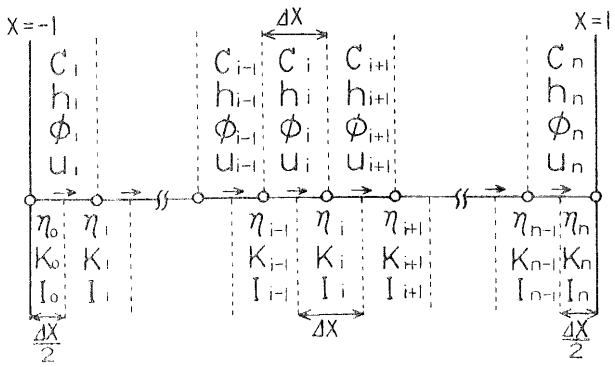

Fig. 4 The discretization with respect to x.

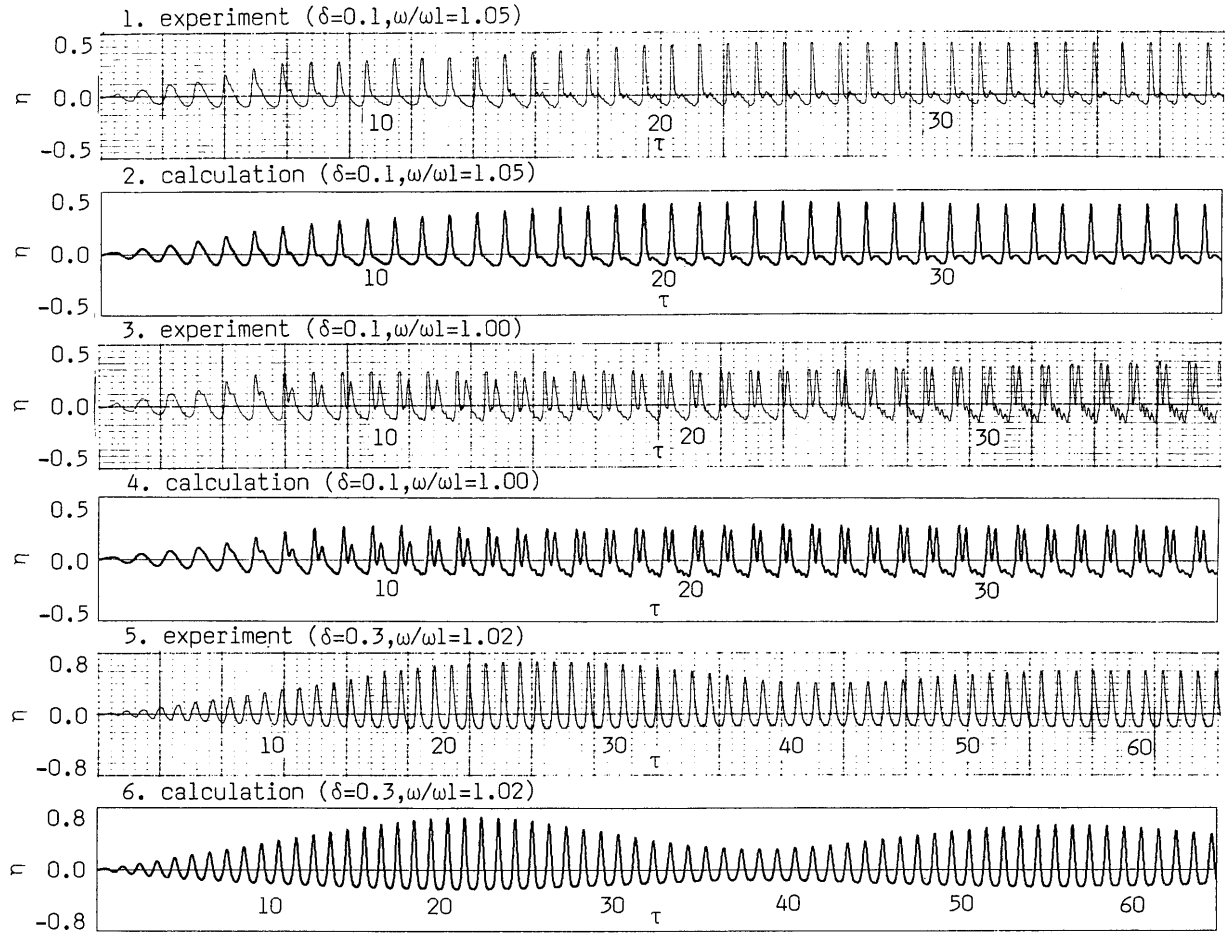

Fig. 5 The typical examples of the transient responses of surface elevation.

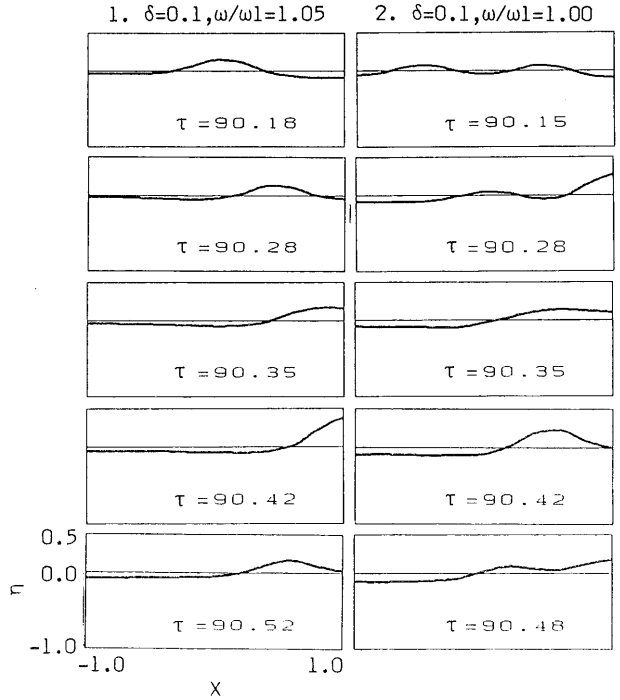

Fig. 6 The changes of the wave forms of free surface by calculation.

harmonically forced tank oscillations τ is defined as,

$$\tau=\omega t/(2\pi) \tag{40}$$

5.3 Results and review

The results obtained by experiments and calculations are expressed with nondimensional variables. The values of ω_1 used to plot the experimental results are calculated from Eq.(24), and those for the numerical results are calculated from Eq.(31).

Typical examples of the transient responses of surface elevation are shown in Fig.5. In the case of $\delta=0.1$ and $\omega/\omega_1=1.05$, it is observed that the amplitude of the oscillation of the first mode is growing. The upward amplitudes are larger than the downward ones, and the wave forms are sharp in the upward direction. In the case of $\delta=0.1$ and $\omega/\omega_1=1.00$, the oscillation of the second mode is generated in addition to the first mode. This phenomenon is observed in the vicinity of the forcing angular frequency which is half the second order natural angular frequency. Furthermore, the same can be observed in the vicinities of a third of the third order natural angular frequency and a quarter of the fourth order one. In the case of $\delta=0.3$

and $\omega/\omega_1=1.02$, beats are observed in the transient responses. It is seen that the peak of the first beat is the largest. This shows that the calculations of the transient responses are very important in estimating the maximum surface elevation. It is also seen that the calculations can simulate experiments very precisely.

Figure 6 shows the change of the wave forms of the free surface which were calculated at specific times during one period of the steady oscillation. In the case of $\omega/\omega_1=1.05$, it is observed that one progressive wave reflects on the side wall. It appears that the wave stood up at the wall and reached its maximum elevation ($\tau=90.42$) during the reflection process. In the case of $\omega/\omega_1=1.00$, two progressive waves are observed. They collide with each other ($\tau=90.42$) and produce the single largest peak of surface elevation. Thereafter, they are again separated into two waves as before, and each wave behaves very stably, without the effects of collision. The same phenomena are also observed in the experiments.

Figures 7 through 9 show the resonant responses of surface elevation measured on the side wall, in which several peaks are observed in all figures. The largest peaks correspond to the first mode sloshing. They clearly show the nonlinear characteristics of ths hardening restoring forces and of the jumping phenomena. The smaller peaks show the resonances of higher order sloshing. For example, at the peak of the m-th order resonance, the forcing angular frequency coincides with the m-th order natural frequency divided by m. The forcing angular frequencies ω/ω_1 at which the higher mode resonances occur are tabulated in the columns of $\omega_m/\omega_1/m$ in Table 1, where the experimental values are calculated from Eq.(24) and the calculated values from Eq.(33), respectively. The values of $\delta\cdot m$. listed in Table 1 represent the values proportional to the ratio of the liquid depth to wavelength. It is said that the nonlinear characteristics of the hardening restoring force become stronger for smaller values of $\delta\cdot m$.

In conclusion, the results of the calculations are in good agreement with those of the experiments.

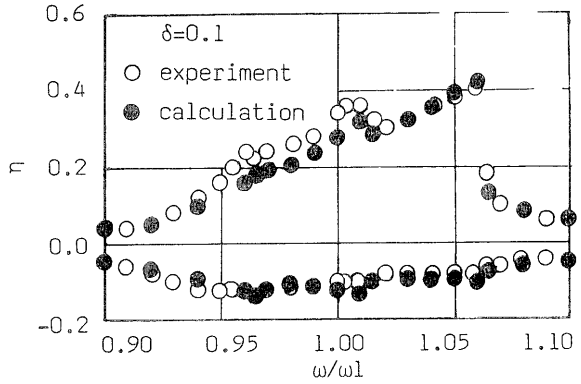

Fig.7 The resonant responses of free surface elevation in case of $\delta=0.1$.

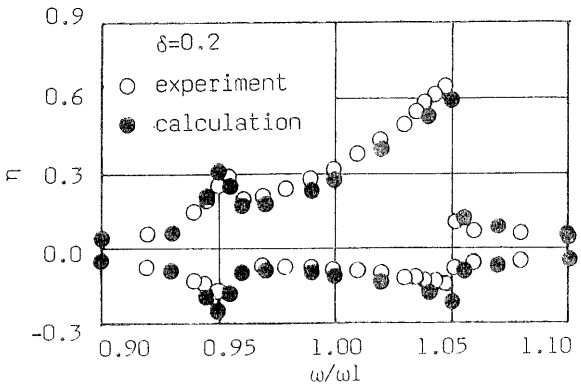

Fig. 8 The resonant responses of free surface elevatios in case of $\delta=0.2$.

6. Conclusions

Based on the shallow water wave theory, the basic equations for describing the nonlinear responses of sloshing in a liquid tank are first derived. Next, a

Table 1 The angularfrequencies causing the higher order resonances.

δ	n	m	experiment (ωm/ω1)/m	calculation (ωm/ω1)/m	δ·m
0.1	10	2	0.988	0.988	0.2
		3	0.969	0.967	0.3
		4	0.945	0.939	0.4
0.2	5	2	0.957	0.951	0.4
0.3	4	2	0.916	0.924	0.6

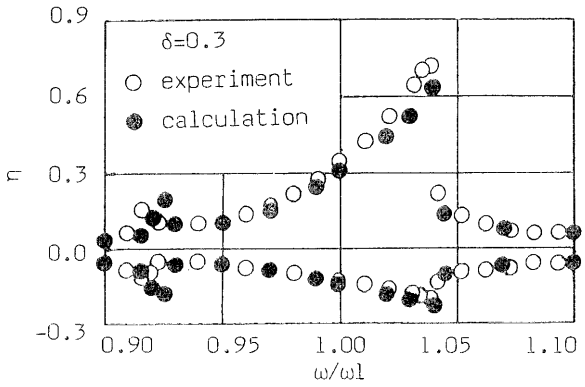

Fig. 9 The resonant responses of free surface elevation in case of $\delta=0.3$.

numerical calculation method is developed to simulate the nonlinear sloshing phenomena in a rectangular tank which is oscillated horizontally. The results of the calculations are compared with those of the experiments. The following results are found.

The linear theory is applicable to simulate the sloshing phenomena with small amplitudes far from resonance. In the vicinity of resonance, however, it is necessary to take the nonlinear characteristics of surface waves into consideration. As the dispersion relation plays an important role for the stable calculations of the nonlinear responses, it should also be taken into consideration. In this study, the dispersion relation is successfully replaced by that produced implicitly by the discretization of the system. Numerical results are in good agreement with those of the experiments. It is confirmed from these facts that, in the cases of shallow liquid depth, the oscillations of the liquid surface are subjected to stable progressive waves, and that the various nonlinear sloshing phenomena observed in a tank with relatively shallow liquid depths are simulated by the basic equations and the calculation method presented in this paper.

References

(1) Moiseev, N. N. and Petrov, A. A., Adv. Appl. Mech., Vol. 9 (1966), p. 91.

(2) Sogabe, K., Inst. Indus. Sci. of Tokyo, (in Japanese), Vol. 26, No. 7 (1974-7), p. 271 ; Vol. 26, No. 9 (1974-9), p. 355.

(3) Fultz, D., J. Fluid Mech., Vol. 13, No. 2 (1962-2), p. 193.

(4) Abramson, H. N., Chu, W. H. and Kana, D. D., Trans. ASME, Ser. E, Vol. 33, No. 4 (1966-12), p. 777.

(5) Hutton, R. E., NASA Tech. Note, D-1870 (1969-5).

(6) Faltinsen, O. M., J. Ship Research, Vol. 18, No. 4 (1974-12), p. 224.

(7) Miles, J. N., J. Fluid Mech., Vol. 75, Pt. 9 (1976), p. 419.

(8) Kimura, N. and Ouhashi, H., Trans. Jpn. Soc. Mech. Eng., (in Japanese), Vol. 44, No. 385(1978-9), p.3024 ; Vol. 44, No. 386 (1978-10), p. 3446 ; Vol. 46, No. 401, C(1980-1), p. 42.

(9) Hayama, S., Aruga, K. and Watanabe, T., Bull. Jpn. Soc. Mech. Eng., Vol. 26, No. 219(1989-9), p. 1641.

(10) Stoker, J. J., Water Waves, (1957), Interscience Publ.

(11) Wiegel, R. L., J. Fluid Mech. Vol. 7, Pt. 2(1960), p. 273.

(12) Hirota, R. and Suzuki, K., J. Phys. Soc. Jpn., Vol. 28, No. 5 (1970), p. 1366 ; Proc. IEEE, Vol. 61, No. 10 (1973-10), p. 1483.